Energy Engineering

Tech Science Press

https://doi.org/10.32604/ee.2026.077594

ARTICLE

# Evaluation of Hydraulic Losses and Photovoltaic Performance in the Design of Solar-Powered Irrigation and Domestic Water Supply Systems for Rural Rwanda

**Aimable Ngendahayo**[1,*], **Adrià Junyent-Ferré**[2] and **Joan Marc Rodriguez Bernuz**[3]

[1]African Center of Excellence in Energy for Sustainable Development, Mechanical Engineering, University of Rwanda-College of Science and Technology, Kigali, Rwanda
[2]Department of Electrical and Electronic Engineering, Imperial College London, London, UK
[3]Departament d'Enginyeria Elèctrica, Universitat Politècnica de Catalunya, Barcelona, Spain

*Corresponding Author: Aimable Ngendahayo. Email: a.ngendahayo@ur.ac.rw

Received: 12 December 2025; Accepted: 03 February 2026; Published: 27 April 2026

**ABSTRACT:** Bugesera, a historically drought-prone region in Rwanda, is undergoing transformation through investment in modern irrigation and sustainable agricultural practices. However, extending the national electrical grid to numerous dispersed smallholder farms poses a major challenge. The persistent water scarcity and rising conventional energy costs necessitate the development of innovative and sustainable solutions. This study investigates the use of photovoltaic (PV) pumping systems as a green energy alternative for off-grid rural areas, supporting both agricultural irrigation and domestic water supply. A model system serving five one-hectare market-gardening plots and 25 inhabitants was analyzed, with a total daily water demand of 300.75 $m^3$/day. A comprehensive technical and economic evaluation was conducted using MATLAB to optimize the system design, including PV array sizing and storage capacity, to ensure reliable operation under defined water and energy demands. A critical component of the analysis was the optimization of the piping network to balance hydrodynamic performance, energy consumption, and overall system cost. For a water requirement of 300.75 $m^3$/day, the optimal PV system consisted of 12 panels, providing a cost-effective balance between energy generation and pumping demand. The results show a rapid decrease in total system cost as the pipe diameter increases from 0.15 to 0.30 m, primarily due to reduced friction losses that lower the total dynamic head and significantly decrease the required PV array size, which dominates the system cost. An optimal diameter of approximately 0.30 m was identified, beyond which further increases yield diminishing cost reductions as the total dynamic head becomes governed mainly by static head rather than hydraulic losses. This integrated technical and economic approach provides a practical framework for designing sustainable, cost-effective solar-powered irrigation and domestic water systems tailored to off-grid smallholder farmers in drought-prone regions.

**KEYWORDS:** Photovoltaic pumping system; techno-economic optimization; total dynamic head; pipe diameter optimization; off-grid water supply; solar-powered irrigation

## 1 Introduction

In today's rapidly evolving world, it is essential to sustainably address issues such as food security and energy access. For small-scale farmers in sub-Saharan Africa, access to irrigation systems is essential for enhancing food availability, boosting earnings, and improving resilience to climate change in rural areas [1]. In remote areas, especially those with limited infrastructure, obtaining a consistent water supply is a significant obstacle to agricultural development. This issue is particularly critical in Rwanda, where most of the population relies on subsistence farming [2]. Irrigation plays a crucial role in countering the risks posed by unpredictable rainfall, extended dry periods, and climate change. Nevertheless, many rural farmers in Rwanda lack the necessary resources and equipment to implement efficient irrigation methods, resulting in poor crop yield and food shortages. Standalone photovoltaic water pumping systems have proven to be a highly competitive solution for water supply in rural regions for irrigation, and they have the potential to transform agricultural practices in poor rural areas by providing a consistent water supply and enabling year-round farming. This is particularly true in areas where connecting to an electric grid is either unfeasible or economically unviable [3]. This study focused on the design and performance of photovoltaic-powered pumping systems for sustainable water supply in rural and off-grid agricultural communities by assessing water demand, hydraulic network parameters, and solar energy requirements to optimize irrigation and domestic water use in smallholder farming areas in the region.

This study explored the appropriate solar-powered pumping system technology that aligns with the socioeconomic and environmental conditions of Rwanda. By leveraging locally available resources and community-driven approaches, this study aims to propose scalable solutions that enhance agricultural productivity and contribute to poverty alleviation in rural areas of the country's western region. Utilizing photovoltaic (PV) arrays for water pumping is among the most promising applications of solar energy, which is a green technology, and solar-powered systems reduce the reliance on fossil fuels [4]. To encourage the use of renewable energy and decrease $CO_2$ emissions, systems that utilize solar energy should be designed [5]. Green energy is a type of energy that is frequently obtained from renewable energy sources, such as the sun, wind, hydroelectricity, geothermal energy, tidal and ocean energy, biomass, and biofuels. Each of these technologies operates differently, whether it is by harnessing solar energy, as with solar panels, or by generating energy through the wind, water flow, or by obtaining energy from the ocean's surface waves [6,7]. Green energy is fundamental for achieving sustainable development and an environmentally friendly environment. Renewable energy sources are considered green energy sources when they have zero impact on the environment, that is, they do not emit any greenhouse gases or emit only a very small amount [8].

One of the most basic issues in confined fluid flow is energy loss, specifically the calculation of pressure drops and the description of the flow form, which contribute to the factors that hinder the performance of PV piping systems [9]. The simplest configuration (Fig. 1) of a solar water pumping system for irrigation includes a solar photovoltaic array, water pump, and water tank. When solar light energy strikes the contactors, the flow of electrons completes the circuit. The electrical energy of PV panels can be used to operate motors to pump groundwater for irrigation purposes. The pumped water can be stored in tanks for future use. The operation of the pump is controlled by a pump controller that assesses the voltage output of the panels [10].

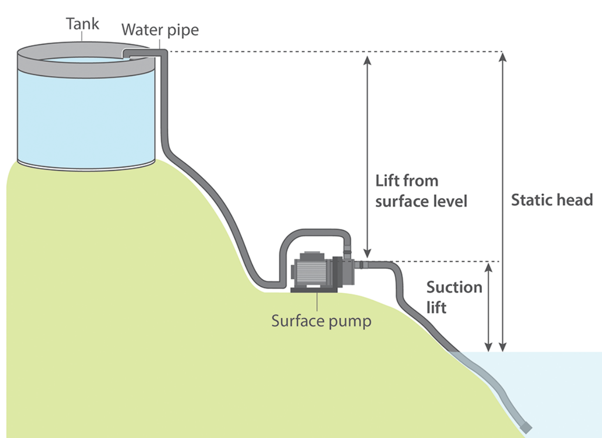


**Figure 1:** Surface sun powered schemes with Static Head [11].

***Case Study***

Pumping water for irrigation from the stream to the tank located in the NTARAMA sector KIBUNGO Cell in Kagoma II village, Fig. 2. When examining the climate of the Bugesera region in relation to other areas, it is characterized by dry conditions with temperatures fluctuating between 20°C and 30°C. The typical temperature range is 26°C–29°C. Previously, the district was transformed into a desert-like area. Nevertheless, owing to increased government initiatives, the district has undergone reforestation and safeguarded its natural resources. This intervention has led to enhanced climatic conditions [12]. Bugesera has the highest annual average solar irradiance of 5.28 kWh/m$^2$_day, with almost 5 h of maximum sunlight daily, solar energy systems could provide a plentiful and consistent power source when properly utilized [13,14].


**Figure 2:** Kagoma-II village [12].

The tank was located 600 m from the local river, with a suction head of 4 m a Static discharge head of 21 m. The hill does not have a high inclination and is likely to be hilly with a moderate slope. The water needs to be pumped and stored during the sunny time, and the duration for pumping is 5 h/day (9 a.m. to 2 p.m.). In this case, irrigation was performed using gravitational irrigation to minimize costs. Currently, the most common way to pump water in the region is by using electricity from the grid and diesel-dependent pumps. Most of this grid electricity comes from non-renewable sources, as renewables have not yet been fully implemented. However, connecting a water-pumping system to the nearest electric grid is not always feasible because of the high cost of extending the main grids. Consequently, renewable energy systems have become a suitable and cost-effective solution for supplying electricity to remote areas [14]. For sub-Saharan Africa, the water requirements can be estimated as follows: Humans: Person 5 to 10 L/day minimum, normal living conditions 30 L/day, market gardening agriculture 60 m$^3$/hectare/day for 1 ha [15].

In this study, the water requirement for market gardening agriculture was estimated to be 60 m$^3$ per hectare per day. Five farmers were considered, each cultivating 1 ha of land, resulting in a total irrigation demand of 300 m$^3$/day. Domestic water needs were incorporated using a standard consumption rate of 30 L per person per day. Based on Table 1, the total number of people considered across the five households was 25, corresponding to a combined domestic water requirement of 750 L/day (0.75 m$^3$/day) per household. Therefore, the total daily water demand for the study area was 300.75 m$^3$/day. In addition, the storage system was sized to ensure the reliable and productive operation of the water-pumping system. This study also evaluated local irrigation systems by analyzing the main parameters affecting hydraulic network performance and determining the necessary water volume and solar panel size required for optimal system efficiency.

**Table 1:** Domestic water requirement estimation based on household population.

| Household | Number of Persons | Water Requirement (L/day) | Water Requirement ($m^3$/day) |
|---|---|---|---|
| Farmer 1 | 5 | 150 | 0.15 |
| Farmer 2 | 8 | 240 | 0.24 |
| Farmer 3 | 6 | 180 | 0.18 |
| Farmer 4 | 4 | 120 | 0.12 |
| Farmer 5 | 2 | 60 | 0.06 |

Water pumping Solar-powered water pumping systems have been widely recognized as sustainable solutions for irrigation and domestic water supply in off-grid rural areas. Several studies have demonstrated the technical and economic feasibility of photovoltaic (PV) water pumping (PVWP) systems using various simulation and modeling tools. For instance, models developed with PVsyst and HOMER software have been successfully applied to assess the practical and economic viability of solar-powered water pumping systems, showing promising results for implementation at sites with similar environmental conditions [16,17]. Similarly, simulation analyses using specialized tools like the Solar-Drip Simulation Tool (SoSiT) have reinforced the potential of PVWP systems as environmentally friendly and sustainable alternatives for irrigation in rural communities lacking grid access [18].

Beyond feasibility, optimization of system design parameters, such as PV module tilt angle, shading effects, and pump sizing, has been explored using platforms such as PVGIS and MATLAB/Simulink. Studies employing PVGIS have highlighted how optimal module orientation and shading analysis can significantly improve water supply efficiency, fulfilling crop irrigation requirements while minimizing resource waste [19]. In parallel, MATLAB/Simulink models incorporating both AC and DC motor pump configurations have enabled precise PV dimensioning tailored to specific farm requirements, suggesting PVWP systems' multi-faceted benefits including rural quality of life improvement and environmental conservation [20]. Further, research employing CROPWAT simulation software has compared PVWP systems to diesel-powered alternatives, underscoring the long-term economic advantages of solar solutions for crop irrigation [21].

Operational and economic aspects, including storage and system reliability, have been addressed in previous studies. For example, the dynamic modeling of groundwater extraction systems integrating battery storage and water tanks demonstrated improved economic viability for dry-season irrigation in Bangladesh [22]. Additionally, comparative numerical sizing methods considering solar cell temperature variations influenced by ambient temperature and wind speed have refined energy consumption models, enhancing the accuracy of PV system performance predictions [23]. In the Rwandan context, several site-specific studies have begun to address the application of PV water-pumping systems under local climatic and operational conditions. A study conducted in Mibirizi village presented the design and technical evaluation of a solar-powered water pumping system, demonstrating the feasibility and reliability of PV technology for rural water supply in Rwanda [24]. At a broader scale, a recent nationwide assessment evaluated the spatial suitability of PV-powered irrigation systems across Rwanda, highlighting the country's high solar irradiation potential and the influence of regional climatic conditions on system design. The study reported that Rwanda's maximum ambient temperature ranges between 25 and 27.5°C throughout the year, indicating favorable operating conditions for PV irrigation systems with minimal thermal losses affecting PV performance [25]. Furthermore, environmental and economic analyses conducted for agricultural irrigation in the Bugesera District using HOMER software compared photovoltaic, diesel, and hybrid pumping systems, revealing that PV water pumping systems are the most cost-effective and environmentally sustainable option for smallholder farming applications in Rwanda [26].

Despite these significant contributions, most previous studies, both globally and within Rwanda, have primarily focused on system feasibility, energy yield estimation, and economic comparisons. A detailed and systematic evaluation of how key hydraulic and operational parameters, particularly hydraulic losses within the water distribution network, influence the overall PV system performance and reliability remains largely unexplored. Moreover, the interaction between hydraulic losses and photovoltaic performance under site-specific rural Rwandan conditions has not been sufficiently addressed in the literature. Accordingly, this study seeks to fill this gap by comprehensively evaluating the main hydraulic and operational parameters affecting the efficiency and reliability of PV-powered irrigation and domestic water supply systems in rural areas of Rwanda. By integrating hydraulic loss analysis with photovoltaic performance assessment, this study provides a context-specific framework for optimizing green energy utilization in off-grid smallholder farming communities.

## 2 Electro-Mechanical System Sizing

Determining the dimensions of photovoltaic water pumping systems (PVWPS) involves several calculations, including the assessment of pump hydraulic power, motor power, photovoltaic array dimensions, and system configurations. Hydraulic energy loss estimation is a critical aspect of fluid dynamics and water resource management because it directly impacts the efficiency of hydraulic systems [27]. The hydraulic power of a water-pumping system is determined by two key factors: the designed head ($H$, measured in meters) and the water flow rate ($Q$, measured in cubic meters per hour). To calculate the hydraulic power required for the pumping system, a specific equation (Eq. (1)) was used [28].

$$P_H\,(\mathrm{kW}) = \frac{H \times Q \times \rho \times g}{3.6 \times 10^6} \tag{1}$$

where $g$ is the acceleration due to gravity (9.81 m/s$^2$), $\rho$ is the water density (kg/m$^3$), and $H$ is the total dynamic head (m). In the flow of a real fluid, the energy always decreases in the flow direction and is dissipated owing to friction losses as the flow traverses through pipe systems. Fluid flow experiences two primary types of head loss. The first type, known as "major losses" or friction head loss, as shown in Eq. (2), is related to the energy dissipation per unit length of the pipe. Typically, turbulent flows with high Reynolds numbers tend to lose energy. The second type, referred to as "minor losses" or local head loss in Eq. (5), results from various factors that obstruct the flow path, such as bends, fittings, valves, and other impediments [29]. When water moves from a river to a tank, both of which are essentially static reservoirs at atmospheric pressure, the pump must provide sufficient energy to the water to overcome two factors: the gravitational head, which is the change in elevation, and the head losses, which include both major and minor losses [30]. The Darcy–Weisbach equation (Eq. (2)) is the most important theoretical model for estimating the frictional energy losses ($h_f$) in pipes by considering the average fluid velocity ($\boldsymbol{U_m}$) and frictional resistance [31]. Many engineers regard the Darcy-Weisbach equation as the most precise method for calculating friction losses in fluid flow systems [32]. It is primarily employed to determine the head loss caused by friction in turbulent flow conditions

$$h_f = f\frac{L}{D}\frac{\boldsymbol{U_m^2}}{\boldsymbol{2g}} \tag{2}$$

where $L$ is the length of the pressurized conduit, $D$ is Pipe diameter, $\boldsymbol{g}$ is the acceleration due to gravity, and $f$ is the friction factor. In cylindrical pipes, the friction factor is typically determined using a Moody diagram. This diagram depicts the Reynolds number against the friction factor and describes the corresponding fluid [33,34]. The friction factor $f$ depends on the Reynolds number, as in the case of laminar flow, as well as on the coefficient of the relative roughness, the relationship between the absolute roughness of the pipe's inner wall surface in contact with the fluid, and the diameter of the pipe ($\varepsilon$/d), considering that the pipe can either perform as a smooth, rough, or somewhere in between. Conversely, The Colebrook-White equation, recognized as the most precise method for determining Darcy's friction factor, provides implicit Eq. (3), in which the friction factor appears on both sides of the equation and therefore requires iterative numerical methods [35,36].

$$\frac{1}{\sqrt{f}} = -2\log_{10}\left(\frac{\varepsilon}{3.72D} + \frac{2.51}{Re\sqrt{f}}\right) \tag{3}$$

Several explicit approximations have been proposed to simplify the evaluation of the Darcy-Weisbach friction factor without the need for iterative solutions. Among the most widely used is the Swamee-Jain explicit equation (Eq. (4)), which provides an accurate approximation of the implicit Colebrook-White equation suitable for engineering applications [37]. The reliability and comparative performance of various explicit formulations, including the Swamee-Jain equation, have been recently reviewed in the literature, demonstrating their effectiveness in head loss estimation and hydraulic design problems [38]

$$f = \frac{0.25}{\left[\log_{10}\left(\frac{\varepsilon}{3.72D} + \frac{5.74}{Re^{0.9}}\right)\right]^2} \tag{4}$$

Typically, the hydraulic head or total dynamic head (H) comprises three primary components: static head ($TDH_{base}$) in Fig. 1 and friction losses [39]. These elements are combined as shown in Eq. (5).

$$H = TDH_{base} + h_f + h_m \tag{5}$$

where $h_m$ accounts for minor losses which they bring extra load losses that can be evaluated using the formula in Eq. (6).

$$H_m = (K_1 + K_2 + (n \times K_3)) \times \frac{U_m^2}{2 \times g} \tag{6}$$

where $n$ is the number of 90° elbows, $K$ is the minor loss coefficient related to the component type, and $U_m$ is the mean flow velocity. Table 2 [40] lists the different $K$ values for different types of minor losses in this study. Including $K_1$ and $K_2$, which correspond to the pipe exit and entrance coefficients, respectively. The coefficient $K_3$ relates to the 90° elbow, with $n = 2$ representing the number of such fittings considered in the system.

**Table 2:** Friction coefficient values.

| Type | *K* |
|---|---|
| Exit (pipe to tank) | 1.0 |
| Entrance (tank to pipe) | 0.5 |
| 90° elbow | 0.9 |
| 45° elbow | 0.4 |
| T-junction | 1.8 |
| Gate valve | 0.25–25 |

### 2.1 Motor Power Calculation

Surface and submersible water pumps are typically installed for irrigation in the agricultural sector. Many PV water pumping systems employ DC motors (instead of AC motors) because they can be directly coupled with PV arrays, resulting in a very simple system. Among the different types of DC motors, a permanent magnet DC (PMDC) motor is preferred in PV systems because it can provide a higher starting torque [41]. The power required by the motor ($P_m$) is calculated using Eq. (7) and depends on the efficiency of the water pump ($\eta_{MP}$). In this research, a constant pump efficiency of 0.56 was used based on [42], to represent the best efficiency point (BEP) of the selected pump class

$$P_m = \frac{P_H}{\eta_{MP}} \text{ [kW]} \tag{7}$$

### 2.2 Photovoltaic Panel Sizing

For solar photovoltaic WPS, the photovoltaic system depends on the power required by the induction motor, system efficiency, and the daily water requirement. The photovoltaic power requirement per day for the water pumping system was calculated using Eq. (8) [43,44]. To calculate the required PV energy, the total watt-hours per day were multiplied by 1.3 (system loss) and divided by the panel generation factor (4.35 for Rwanda) [10]. The system is designed to run for only 5 h during the daytime (9 a.m.–2 p.m.). The rated power of the PV modules to be used is 500 Wp, which is available on the Rwandan market, and the designed number of PV panels is 36.

$$P_{PV} = \frac{P_m \times h \times 1.3}{4.35} \tag{8}$$

### 2.3 Storage Battery Sizing

This section describes the method used to determine the suitable size of the storage battery. The battery storage system (BSS) should be sufficiently large to store sufficient energy to operate the PV station at night and on cloudy days. The required storage was sized using Eq. (9) [45]. Given a battery efficiency of 0.85, depth of discharge (DOD) of 0.85, and battery voltage of 72 volts, the system can operate for one day without power generation from the photovoltaic (PV) panels. The calculated energy capacity was 341.64 Ah.

$$BSS(\text{Ah}) = \frac{\text{Total watt} - \text{hours per day} * \text{Day of autonomy}}{battery\ efficiency * DOD * Battery\ voltage} \tag{9}$$

The batteries considered for this application are retired electric vehicle (EV) batteries that have been repurposed for secondary use in BESSs. An EV battery is typically deemed to have reached the end of its primary life cycle when its capacity or State of Health (SOH) falls to approximately 80% of the original nominal capacity [46]. At this threshold, the battery is no longer suitable for high-performance automotive applications, primarily because of the diminished driving range and reduced peak power delivery caused by increasing internal resistance. However, the remaining 70%–80% capacity still constitutes a high-value energy asset that can serve effectively for an additional 5 to 10 years in less demanding applications, such as stationary energy storage [47,48]. After calculating the required number of PV panels, the next step is to analyze the cost to gain a deep understanding of the effect of the main PV pumping parameters on the total cost. The cost analysis and viability of clean energy infrastructure are key considerations in promoting sustainable urban mobility. Thus, conducting a comprehensive economic assessment is crucial to determine the project's feasibility, considering the costs associated with installing PV generation, BESS, and battery pumping systems [49]. The total cost of the system ($C_{total}$) in Eq. (10) depends on the PV array cost ($C_{PV}$), pump cost ($C_{pump}$), pipe cost ($C_{pipe}$), and battery transport and collection cost ($C_{b\_col}$) [50].

$$C_{total} = C_{PV} + C_{pump} + C_{pipe} + C_{b\_col} \tag{10}$$

The pipe cost was calculated from the pipe cost per meter, which is 0.5$ and the total length, panel cost for one panel is 182$. The considered pump cost is 60$ and the one for second use battery transportation is 0.1$. Subsequently, the pipe size that minimized the overall expenses was determined. This optimal diameter was identified by assessing the total cost of the pumping system for various pipe sizes. The expenses associated with each pipe diameter were calculated and compared. The size that yielded the lowest overall cost was selected as the ideal size for the specified pumping requirements. This method ensures that the system is economical and capable of supplying the necessary water volumes.

## 3 Results and Discussions

Fig. 3 shows the number of photovoltaic (PV) panels required for a solar-powered irrigation system, considering two critical factors: the amount of water needed per hectare for irrigation (Nwh) and the Total Dynamic Head (TDH). An increase in Nwh signified a greater volume of water to be pumped daily, which required more energy to operate the pump.

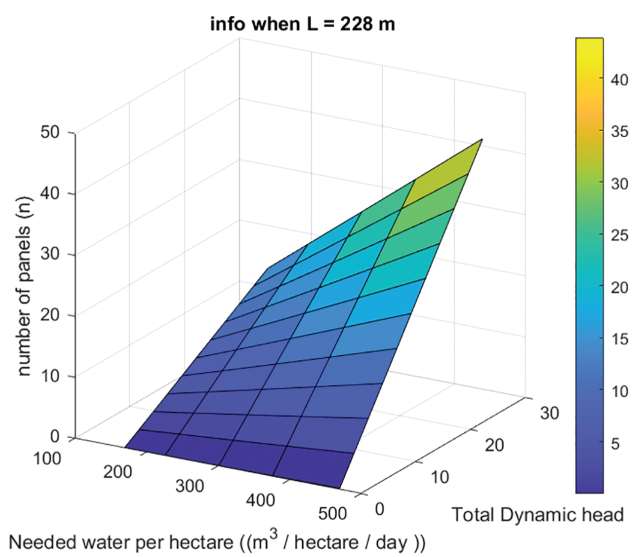


**Figure 3:** Number of PV panels with respect to needed water and total dynamic head.

Because PV panels are the energy source, more panels are required to meet the higher energy demand. Conversely, a lower Nwh reduces the energy requirement, resulting in fewer PV panels being required. TDH represents the vertical height and resistance that the pump must overcome to lift water. A higher TDH increases the power required by the pump, thereby necessitating a larger solar array. This is because the energy demand increases as the TDH increases, owing to higher gravitational and frictional losses. As both Nwh and TDH increase, the energy demand of the system increases, necessitating additional PV panels to ensure reliable operation.

The next parameter to be analyzed was the hydraulic losses in the fluid flow, as shown in Fig. 4. Increasing the diameter reduces the losses owing to the lower flow velocity at the same flow rate, thereby resulting in less friction. Large-diameter pipes are beneficial for minimizing energy losses but are more expensive in terms of materials. Higher velocities cause greater turbulence and friction, thereby amplifying energy losses. Controlling the velocity is crucial for maintaining the efficiency. Balancing the diameter and velocity is essential for system design. Oversized pipes reduce losses but increase costs, whereas higher velocities minimize the pipe size but increase the energy expenses. Thus, optimizing these parameters ensures a cost-effective and efficient hydraulic-system design.

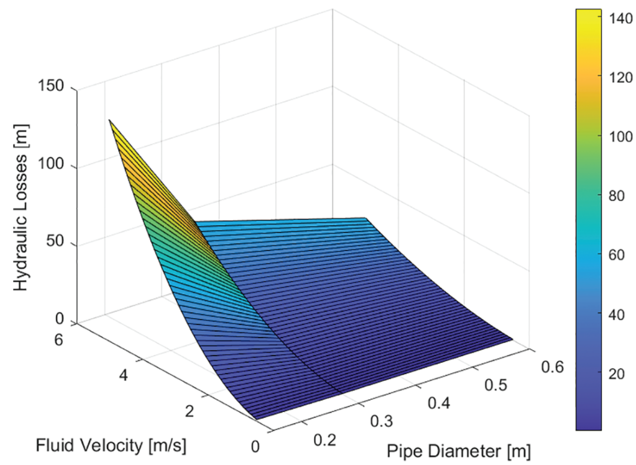


**Figure 4:** Hydraulic losses vs. diameter and fluid Velocity.

The results presented in Fig. 5 indicate a pronounced decrease in the total system cost as the pipe diameter increases from 0.15 to 0.30 m. This behavior is primarily attributed to the strong sensitivity of the hydraulic losses to the pipe diameter. Specifically, the flow velocity decreases proportionally to $1/D^2$, whereas the Darcy-Weisbach friction losses decrease approximately with $1/D^5$ [31]. Consequently, doubling the pipe diameter from 0.15 to 0.30 m yields an approximate 32-fold reduction in friction losses, which significantly decreases the Total Dynamic Head (TDH) [51,52]. Reduced TDH leads to lower pump hydraulic power and electrical energy requirements, thereby decreasing the size and number of photovoltaic (PV) panels required. Because the PV subsystem constitutes the dominant component of the overall system cost, reductions in energy demand translate directly into substantial cost savings within this diameter range. Beyond 0.30 m, the cost curves in Fig. 5 exhibit a diminishing rate of decrease.

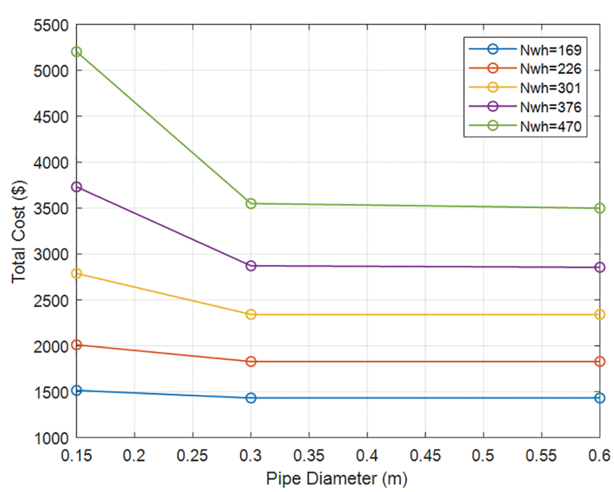


**Figure 5:** Total cost vs. pipe diameter for different water needs.

This trend occurs because once the friction and minor losses become relatively small, the TDH is governed mainly by the static head, limiting further reductions in the pump energy consumption. In this case, the principal cost contributors, namely the pump and PV array, dominate the system cost, and further increases in the pipe diameter offer only marginal improvements in hydraulic performance. Additionally, although larger pipe diameters increase the material cost, the magnitude of this increase is negligible compared to the cost of the pump and PV subsystems. Consequently, enlarging the pipe diameter beyond approximately 0.30 m provides diminishing economic benefits, and the cost curve asymptotically approaches a minimum dictated by components that are insensitive to the pipe diameter.

The final key parameter evaluated in this study was the optimization of the number of photovoltaic (PV) panels necessary to satisfy the designed daily water demand. As illustrated in Fig. 6, for a water requirement of 300.75 $m^3$/day per hectare, the optimal number of PV panels was determined to be 12, balancing the energy generation capacity with the system efficiency and cost-effectiveness.

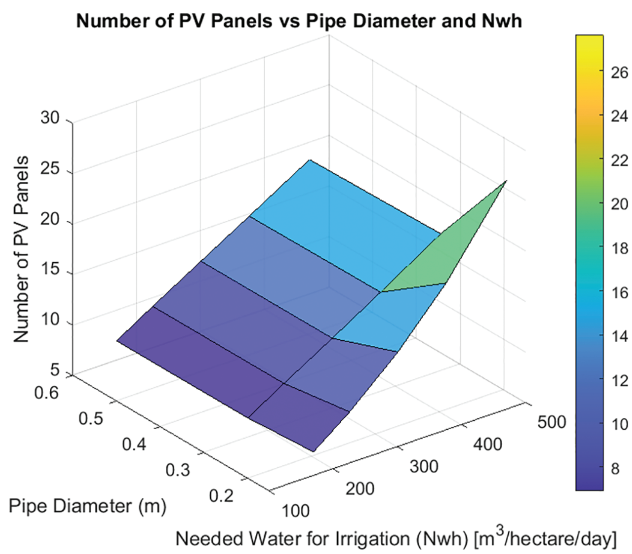


**Figure 6:** Number of PV panels vs. pipe diameter and required water.

## 4 Analysis and Critical Assessment

This study was developed to support communities in remote areas of Rwanda by providing knowledge on how solar PV technology can be applied in PV water-pumping systems to promote the productive use of green energy efficiently. As shown in Fig. 3, an increase in water demand corresponds to a higher volume of water that must be pumped daily, which, in turn, requires more energy to operate the pump. Because the energy supply comes from PV panels, meeting this increased energy requirement necessitates additional panels, thereby raising the overall system cost, as demonstrated in [53]. The authors highlighted that fewer PV panels result in lower installation costs and reduced energy waste. This study further shows that higher energy consumption is influenced by the characteristics of the piping system, as illustrated in Fig. 4. Increasing the pipe diameter reduces the head losses because a larger cross-sectional area lowers the flow velocity for a given discharge, thereby reducing the friction. Although large-diameter pipes effectively minimize hydraulic losses, they are associated with higher costs. Conversely, high flow velocities generate greater turbulence and friction, increasing energy losses, as supported by [54]. Increasing the pipe diameter reduces the energy dissipation for a fixed flow rate by lowering the velocity and wall shear stress; however, larger pipes also increase the initial capital cost for materials and installation [55].

This creates an inherent economic tradeoff. Designs that maintain moderate velocities and thus reduce long-term pumping energy and turbulence losses are generally more cost-effective over the lifetime of the system. In contrast, high-velocity, small-diameter designs may reduce initial capital expenditure but tend to incur higher operational costs unless the system has a short operating period or the project is severely constrained by the budget [56]. Therefore, the authors recommend avoiding sustained high velocities in pipe design unless justified by a life-cycle cost analysis or limited operational duration. This study identified an optimal pipe diameter of approximately 0.30 m, balancing both cost and hydraulic losses. As demonstrated in Fig. 5, increasing the pipe diameter beyond 0.30 m provides little additional economic benefit, as the cost curve flattens and approaches a lower limit determined by the system components that are not sensitive to the pipe diameter. This aligns with previous research emphasizing the importance of adjusting the pipe diameter to achieve optimal network performance [57]. This research significantly contributes to the field by offering practical and relevant results for optimizing and designing PV water-pumping systems in the context of rural energy development for the productive use of green energy. This provides a robust basis for subsequent studies and real-world deployment.

## 5 Conclusion

This study addressed the energy access challenges faced by remote communities for irrigation and domestic water supply through the development and analysis of a photovoltaic (PV) pumping system. The system was modeled and optimized using MATLAB, focusing on affordable PV system sizing and an efficient piping network design. A comprehensive model was presented to optimize the pipe diameter in PV pumping systems by integrating hydrodynamics, PV generation, and economic considerations.

The results demonstrated that the system's energy demand and total cost increase significantly with higher irrigation water requirements (Nwh) and total dynamic head (TDH), necessitating larger PV arrays and raising overall costs. Hydraulic losses were shown to decrease sharply as the pipe diameter increased from 0.15 to 0.30 m owing to the reduced flow velocity and friction, resulting in significant cost savings within this range. The optimal pipe diameter was identified as approximately 0.30 m, which minimized the total system cost for the studied case. For pipe diameters exceeding 0.30 m, the system approaches a cost-performance plateau, where hydraulic losses become minimal, and the TDH is largely influenced by the static head. Beyond this point, further increases in pipe diameter yielded only marginal efficiency improvements while material costs continued to rise. This regime yields only marginal efficiency improvements, while material costs continue to rise. In conclusion, balancing hydraulic parameters with energy requirements is critical for designing cost-effective and energy-efficient solar-powered irrigation systems. The proper selection of pipe diameter, pump capacity, and PV array size tailored to site-specific Nwh and TDH conditions ensures sustainable operation with minimized energy consumption and overall system cost.

In this study, pump efficiency ($\eta_{MP}$) was assumed constant at 0.56 based on typical manufacturer data [43]. While this simplification allowed for a focused analysis of system-level performance and cost, it is well known that pump efficiency varies with operating conditions such as volumetric flow rate and total dynamic head. To improve model accuracy and better reflect real-world pump behavior, future work should incorporate a variable pump efficiency model that accounts for these dependencies.

**Acknowledgement:** The authors of this paper would like to thank the Engineering and Physics Sciences Research Council (UK) under the Project "RENGA: Resilient Electricity Networks for a Productive Grid Architecture" from the Imperial College of London, UK for their support. Furthermore, the authors acknowledge important support from the African Center of Excellence Energy for Sustainable Development located at the University of Rwanda, College of Science and Technology (UR-CST).

**Funding Statement:** This study was supported by the Global Challenges Research Fund (GCRF) through the Engineering and Physical Sciences Research Council UK under project RENGA (EP/R030235/1). It was also funded by the African Center of Excellence in Energy for Sustainable Development (ACE-ESD) under the University of Rwanda, College of Science and Technology.

**Author Contributions:** The authors confirm their contribution to the paper as follows: study conception and design, Adrià Junyent-Ferré, Aimable Ngendahayo; data collection: Aimable Ngendahayo, Adrià Junyent-Ferré; analysis and interpretation of results: Aimable Ngendahayo, Joan Marc Rodriguez Bernuz; methodology: Aimable Ngendahayo, Adrià Junyent-Ferré; software: Joan Marc Rodriguez Bernuz, Adrià Junyent-Ferré; draft manuscript preparation: Aimable Ngendahayo; supervision: Adrià Junyent-Ferré, Joan Marc Rodriguez Bernuz; project administration: Adrià Junyent-Ferré. All authors reviewed and approved the final version of the manuscript.

**Availability of Data and Materials:** The data used to support the findings of this study are available from the corresponding author upon request.

**Ethics Approval:** Not applicable.

**Conflicts of Interest:** The authors declare no conflicts of interest.

## References

1. Akaliza N, Bodnar L, Brozovic N, Mukarusagara G, Turatsinze F, Urujeni R. Current state of irrigation-as-a-service for smallholder farmers in Rwanda. Lincoln, NE, USA: Daugherty Water for Food Global Institute; 2023. 22 p.
2. Geoffrey G, de Dieu MJ, Pierre NJ, Aimable T. Design of automatic irrigation system for small farmers in Rwanda. Agric Sci. 2015;6(3):291–4. doi:10.4236/as.2015.63029.
3. Shebani MM, Iqbal T. Dynamic modeling, control, and analysis of a solar water pumping system for Libya. J Renew Energy. 2017;2017(1):8504283. doi:10.1155/2017/8504283.
4. Anka P, Raghavendra V, Palled V, Veerangouda M. Performance evaluation of solar water pumping system. Int J Curr Microbiol App Sci. 2018;7(5):133–42. doi:10.20546/ijcmas.2018.705.017.
5. Mishra S, Dwivedi G, Upadhyay S, Chauhan A. Modelling of standalone solar photovoltaic based electric bike charging. Mater Today Proc. 2022;49(2):473–80. doi:10.1016/j.matpr.2021.02.738.
6. Sharma VK, Monteleone G, Braccio G, Anyanwu CN, Aneke NN. A comprehensive review of green energy technologies: towards sustainable clean energy transition and global net-zero carbon emissions. Processes. 2025;13(1):69. doi:10.3390/pr13010069.
7. IRENA, The World Bank. TRACKING SDG7: the emergy progress report. Washington, DC, USA: IRENA/The World Bank; 2019. 176 p.
8. Androniceanu A, Sabie OM. Overview of green energy as a real strategic option for sustainable development. Energies. 2022;15(22):8573. doi:10.3390/en15228573.
9. Berrada A, Loudiyi K. System performance and testing. In: Gravity energy storage. Amsterdam, The Netherlands: Elsevier; 2019. p. 105–39. doi:10.1016/b978-0-12-816717-5.00005-0.
10. Biswas S, Iqbal MT. Dynamic modelling of a solar water pumping system with energy storage. J Sol Energy. 2018;2018(3):8471715. doi:10.1155/2018/8471715.
11. World Bank. Solar water pumping systems system design, selection and installation guidelines. Washington, DC, USA: World Bank; 2017.
12. Hategekimana P, Ferre AJ, Ntagwirumugara E, Bernuz JMR. Assessment of feasible DC microgrid network topologies for rural electrification in Rwanda: studying the Kagoma village. In: Proceedings of the 2020 International Conference on Smart Grids and Energy Systems (SGES); 2020 Nov 23–26; Perth, Australia. p. 854–9. doi:10.1109/sges51519.2020.00157.
13. Bakundukize A, Twizerimana M, Bernadette D, Pierre BJ, Theoneste N. Design and modelling of PV power plant for rural electrification in Kayonza, Rwanda. J Energy Res Rev. 2021;7(4):31–55. doi:10.9734/jenrr/2021/v7i430197.

14. Batalla GH, Parellada AU, Beyer H, Bergsmark S. Water Supply in Rwanda. Use of photovoltaic systems for irrigation [master's thesis]. Kristiansand, Norway: University of Agder; 2015.
15. Hadidi A, Berbaoui I, Saba D. Steps design of a solar station (the solar pumping). In: Proceedings of the Nineteenth International Water Technology Conference, IWTC19; 2016 Apr 21–23; Sharm El Sheikh, Egypt.
16. Ahmed O, Iqbal M. Design of a solar-powered water pumping system for irrigation in Sukkur, Pakistan. Jordan J Electr Eng. 2023;9(1):84. doi:10.5455/jjee.204-1669679136.
17. Sharma R, Sharma S, Sharma S. Techno-economic analysis of solar powered water pumping system. Int J Soft Comput Eng. 2020;9(5):24–32. doi:10.35940/ijsce.e3343.019520.
18. Habib S, Liu H, Tamoor M, Zaka MA, Jia Y, Hussien AG, et al. Technical modelling of solar photovoltaic water pumping system and evaluation of system performance and their socio-economic impact. Heliyon. 2023;9(5):e16105. doi:10.1016/j.heliyon.2023.e16105.
19. Miran S, Tamoor M, Kiren T, Raza F, Hussain MI, Kim JT. Optimization of standalone photovoltaic drip irrigation system: a simulation study. Sustainability. 2022;14(14):8515. doi:10.3390/su14148515.
20. Al-Badi A, Yousef H, Al Mahmoudi T, Al-Shammaki M, Al-Abri A, Al-Hinai A. Sizing and modelling of photovoltaic water pumping system. Int J Sustain Energy. 2018;37(5):415–27. doi:10.1080/14786451.2016.1276906.
21. Nasir A. Design and simulation of photo-voltaic water pumping system for irrigation. Adv Appl Sci. 2019;4(2):59. doi:10.11648/j.aas.20190402.14.
22. Biswas SB. Sizing, dynamic modelling and control of a solar water pumping system for irrigation [Online]. [cited 2025 Jan 1]. Available from: https://research.library.mun.ca/13351/1/thesis.pdf.
23. Mbow B, Sadio A, Fankam BT, Mbodji S. Optimal sizing of a solar water pumping system for Koyli Alpha village. Senegal Int J Power Electron Drive Syst. 2022;13(2):1158. doi:10.11591/ijpeds.v13.i2.pp1158-1169.
24. Nshimyumuremyi E. Solar water pumping system in isolated area to electricity: the case of Mibirizi village (Rwanda). Smart Grid Renew Energy. 2015;6(2):27–39. doi:10.4236/sgre.2015.62003.
25. Shumbusho JB, Ndungutse F, Niyonsaba M, Gedeon B, Agness M, Fabien N, et al. Suitability of solar photo-voltaic water pumping system for irrigation in Rwanda. Glob Sci J. 2025;13(3):1846–64. doi:10.11648/j.aas.20190402.14.
26. E. Sciences. Environmental and economic cost analysis of a solar PV, diesel and hybrid PV-diesel water pumping systems for agricultural irrigation in Rwanda: case study of Bugesera district [Online]. 2018 [cited 2025 Jan 1]. Available from: http://repository.pauwes-cop.net/handle/1/241.
27. Yao T. Research on the local head loss coefficient in short-tube hydraulic testing. In: Proceedings of the 2024 3rd International Conference on Applied Mechanics and Engineering Structures (AMES 2024); 2024 May 17–19; Zhuhai, China. Dordrecht, The Netherlands: Atlantis Press International BV; 2024. doi: 10.2991/978-94-6463-473-0_10.
28. Chilundo RJ, Mahanjane US, Neves D. Design and performance of photovoltaic water pumping systems: comprehensive review towards a renewable strategy for Mozambique. J Power Energy Eng. 2018;6(7):32–63. doi:10.4236/jpee.2018.67003.
29. Wang J, Chen R, Yang T, Wei T, Wang X. A computationally-efficient finite element method for the hydraulic analysis and design of subsurface drip irrigation subunits. J Hydrol. 2021;595(1):125990. doi:10.1016/j.jhydrol.2021.125990.
30. Shahid S, Sham Dol S, Hasan AQ, Kassem OM, Gadala MS, Aris MS. A review on electrical submersible pump head losses and methods to analyze two-phase performance curve. Wseas Trans Fluid Mech. 2021;16:14–31. doi:10.37394/232013.2021.16.3.
31. Afzal N. Friction factor directly from transitional roughness in a turbulent pipe flow. J Fluids Eng. 2007;129(10):1255–67. doi:10.1115/1.2776961.
32. Ssenozi I, Larson M, Persson T. Modeling energy losses in the hydraulic system of vombverket water treatment plant. J Water Manag Res. 2016;72:211–27.
33. Savić V, Knežević D, Lovrec D, Jocanović M, Karanović V. Determination of pressure losses in hydraulic pipeline systems by considering temperature and pressure. Stroj Vestn/J Mech Eng. 2009;55(4):237–43. doi:10.4271/arp24b.

34. Ali AR, Salam B, Razzaq ME, Ahamed JU, Hassan T, Karim MF. Effect of density, dynamic viscosity, velocity, and diameter on wall shear stress for turbulent pipe flow. In: Proceedings of the International Conference on Mechanical Engineering and Renewable Energy (ICMERE2019); 2019 Dec 11–13; Chittagong, Bangladesh.
35. Abdulameer LS, Dzhumagulova N, Algretawee H, Zhuravleva L, Alshammari MH. Comparison between Hazen-Williams and Darcy-Weisbach equations to calculate head loss through conveyancing treated wastewater in Kerbala city, Iraq. East Eur J Enterp Technol. 2022;1(1(115)):36–43. doi:10.15587/1729-4061.2022.251385.
36. Wichowski P, Kalenik M, Lal A, Morawski D, Chalecki M. Hydraulic and technological investigations of a phenomenon responsible for increase of major head losses in exploited cast-iron water supply pipes. Water. 2021;13(11):1604. doi:10.3390/w13111604.
37. Patricia D, Rojo G, Duane C, Gaia C, Carlos J, Saad C. Determinação do fator de atrito em diferentes regiões do diagrama de moody. IRRIGA. 2024;8546:68–77. doi:10.15809/irriga.2024v29p68-77.
38. Easa SM, Lamri AA, Brkić D. Reliability-based criterion for evaluating explicit approximations of Colebrook equation. J Mar Sci Eng. 2022;10(6):803. doi:10.3390/jmse10060803.
39. Abdullateef A, Issa A, Sulaiman A, Issa A, Salami M, Onasanya O. Sizing and implementation of a standalone solar photovoltaic system for a three-phase submersible pumping machine considering the techno-economics perspectives: a case of super farm ilorin. Niger J Eng. 2023;30(1):1–10. doi:10.5455/nje.2023.30.01.01.
40. Acakpovi A, Xavier FF, Awuah-Baffour R. Analytical method of sizing photovoltaic water pumping system. In: Proceedings of the 2012 IEEE 4th International Conference on Adaptive Science & Technology (ICAST); 2012 Oct 25–27, Kumasi, Ghana. p. 65–9. doi:10.1109/ICASTech.2012.6381067.
41. Krishnakant, Kulkarni PS. Design and simulation of solar photovoltaic water pumping system. In: 2020 3rd International Conference on Energy, Power and Environment: Towards Clean Energy Technologies; 2021 Mar 5–7; Shillong, India. doi:10.1109/ICEPE50861.2021.9404473.
42. Pump curves|Head, power, efficiency, NPSHR vs flow|HI data tool. [cited 2026 Jan 20]. Available from: https://datatool.pumps.org/pump-fundamentals/pump-curves.html?utm_source=chatgpt.com.
43. Despotović ŽV, Tajdić M. Design, implementation and experimental testing of a hybrid power supply of remote measuring station in the surveillance, alert & warning system (SAWS). Telfor J. 2022;14(1):12–9. doi:10.5937/telfor2201012d.
44. Abo-Khalil AG, Sayed K, Radwan A, El-Sharkawy IA. Analysis of the PV system sizing and economic feasibility study in a grid-connected PV system. Case Stud Therm Eng. 2023;45(2):102903. doi:10.1016/j.csite.2023.102903.
45. Siriwattanapong A, Chantharasenawong C. Electric motorcycle charging station powered by solar energy. IOP Conf Ser Mater Sci Eng. 2018;297:012060. doi:10.1088/1757-899x/297/1/012060.
46. Ngendahayo A, Junyent-Ferré A, Bernuz JMR, Ntagwirumugara E. Itinerary-dependent degradation analysis of a lithium-ion battery cell for e-bike applications in Rwanda. Energy Eng. 2024;121(11):3121–31. doi:10.32604/ee.2024.053100.
47. Li J, He S, Yang Q, Wei Z, Li Y, He H. A comprehensive review of second life batteries towards sustainable mechanisms: potential, challenges, and future prospects. IEEE Trans Transp Electrif. 2022;9(4):4824–45. doi:10.1109/TTE.2022.3220411.
48. Stelter EM, Spancken D, Waldmann T, Hogrefe C, Hein C, Hepp A, et al. Sustainable battery design: holistic recyclable lithium-ion battery system for automotive and following 2nd life stationary use. Energy Tech. 2026;14(1):e202501329. doi:10.1002/ente.202501329.
49. Kayitare M, Athanase Dalson G, Sendegeyad AM. A techno-economical characterization of solar PV power generation in Rwanda: the role of subsidies and incentives. Energy Eng. 2023;120(9):2155–75. doi:10.32604/ee.2023.028559.
50. de Mattos Affonso C, Kezunovic M. Technical and economic impact of PV-BESS charging station on transformer life: a case study. IEEE Trans Smart Grid. 2019;10(4):4683–92. doi:10.1109/TSG.2018.2866938.
51. Afzal N, Seena A, Bushra A. Turbulent flow in a machine honed rough pipe for large Reynolds numbers: general roughness scaling laws. J Hydro Environ Res. 2013;7(1):81–90. doi:10.1016/j.jher.2011.08.002.

52. Colebrook CF, Blench T, Chatley H, Essex EH, Finniecome JR, Lacey G, et al. Correspondence. Turbulent flow in pipes, with particular reference to the transition region between the smooth and rough pipe laws (includes plates). J Inst Civ Eng. 1939;12(8):393–422. doi:10.1680/ijoti.1939.14509.
53. Ngendahayo A, Junyent-Ferré A, Rodriguez-Bernuz JM, Nyeko E, Ntagwirumugara E. Sizing requirements of the photovoltaic charging station for small electrical vehicles. Int J Renew Energy Dev. 2024;13(4):630–8. doi:10.61435/ijred.2024.60120.
54. Blacher D, Harasek M. Optimisation of pipes with constant diameter using the heuristic optimality criterion. Open Res Europe. 2023;3:156. doi:10.12688/openreseurope.15943.1.
55. Ghobadian R, Mohammadi K. Optimal design and cost analysis of water distribution networks based on pressure-dependent leakage using NSGA-II. Appl Water Sci. 2023;13(4):92. doi:10.1007/s13201-023-01888-4.
56. Paudel PP, Adhikari S. Technical feasibility and economic analysis of solar photovoltaic water pumping system for sustainable irrigation in Nepal: a case study. Int J Sustain Eng. 2025;18(1):2590115. doi:10.1080/19397038.2025.2590115.
57. Xu H, Zhang L, Wang X, Han B, Luo Z, Bai B. Improved genetic algorithm for pipe diameter optimization of an existing large-scale district heating network. Energy. 2024;304(1):131970. doi:10.1016/j.energy.2024.131970.